An Iterative Method for Bifurcation-Free Resonant Inductive Power Transfer System Design

Nicola Campagna, Vincenzo Castiglia, Rosario Miceli, Filippo Pellitteri
Department of Engineering
Palermo University
90128 Palermo, Italy
Email: nicola.campagna@unipa.it, vincenzo.castiglia@unipa.it, rosario.miceli@unipa.it, filippo.pellitteri@unipa.it

***Abstract*—The development of electric mobility makes the charging systems one of the main discussed topic. Among the different technologies, Resonant Inductive Power Transfer (RIPT) systems are in deep study. Several aspects, including the choice of coils, the compensation network and the bifurcation phenomenon are necessary for a proper design of the system. In this paper an iterative method for bifurcation-free RIPT system design is provided as a valid solution to the need of accurate models requiring low computational efforts.**

***Index Terms*—wireless charging, resonant inductive power transfer (RIPT), bifurcation, modeling.**

I. Introduction

The development of electric vehicles moves the action field of the research to innovative technologies and solutions in the automotive sector [1], [2]. Among the new enabling technologies, wireless charging is one of the burning issues because of the advantages introduced in terms of facilities and safety [3], [4].

The most widely used wireless transfer systems are the Resonant Inductive Power Transfer (RIPT) ones [5]-[9]. They are based on the inductive coupling between two coils, one acting as a transmitter (primary side), the other acting as a receiver (secondary side). In literature different typologies of coupled coils are presented. The most used are the circular planar, the square and the double D (DD) antennas [10], [11]. In order to maximize the transferred power, capacitive compensation networks are introduced in both primary and secondary sides. The capacitance values of the compensation networks are chosen to ensure the resonance of the system.

Based on the connection between the capacitive network and the coils, four different types of compensation are possible: Series-Series (SS), Parallel-Parallel (PP), Series-Parallel (SP) and Parallel-Series (PS) [12]. The SS systems are preferred because the resonance frequency does not depend on the mutual inductance value [13].

An important aspect that should not be neglected in the design phase of a RIPT system is the bifurcation phenomenon [14]. This phenomenon is related to a condition for which the resonant frequency is not unique. If bifurcation occurs, the primary side current is distorted and the efficiency of the system decreases. Different bifurcation-free design methods are proposed in literature and in most of them, a FEM analysis is carried out [15], [16]. Even though magnetostatic and magnetodynamic analyses through finite elements method are extremely accurate and useful, high computational efforts are required [17].

In this paper an iterative method for bifurcation-free RIPT system design is provided as a valid solution. It is based on the bifurcation-free condition verification through algebraic equations, without involving complex integral-differential equation sets. A DD coils-based SS-compensated system is taken into account. The design algorithm is fully described and verified with a system simulation.

II. Bifurcation phenomenon

In order to perform a maximum power transfer, a capacitive compensation network has to be introduced in both primary and secondary side. Compensation capacitors are sized in order to have a purely real input impedance at the resonance operating frequency. The bifurcation phenomenon is referred to a condition for which the resonance frequency ensuring a Zero Phase Angle (ZPA) between voltage and current at the input terminals is not unique. The number of resonance frequencies depends on the mutual inductance value, on the load conditions, on the compensation topology and on the RIPT system parameters values such as the internal resistance and the self-inductance of the coils and the capacitance of the compensation networks. Among the different compensation typologies, a Series-Series compensation is analyzed.

With reference to Fig.1, for a Constant Current (CC) RIPT system operation, neglecting the internal resistance of both primary and secondary coils R_P and R_S, the

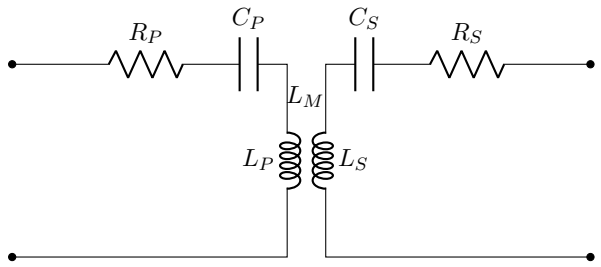

Fig. 1. Series-Series Compensated IPT system equivalent circuit.

expression of the primary resonant circuit impedance $Z_{LP}(\omega)$ and the secondary resonant circuit impedance $Z_{LS}(\omega)$ are

$$\begin{cases} Z_{LP}(\omega) = j\omega L_P + \dfrac{1}{j\omega C_P} \\ Z_{LS}(\omega) = j\omega L_S + \dfrac{1}{j\omega C_S} \end{cases} \tag{1}$$

in which L_P and L_S are respectively the primary side and the secondary side self inductance values, C_P and C_S are respectively the primary side and the secondary side compensation capacitances values and ω is the pulsation.

The secondary side impedance can be calculated as follow:

$$Z_S = Z_{LS} + R_L = j\omega L_S + \frac{1}{j\omega C_S} + R_L, \tag{2}$$

being R_L the load resistance.

The secondary side impedance Z_S can be reported on the primary side. The reflected impedance can be calculated with the following equation:

$$Z_R = \frac{w^2 L_M^2}{Z_S} \tag{3}$$

in which L_M is the mutual inductance value.

Replacing (2) in (3), it is possible to find the expression of the real part and the imaginary part of the impedance Z_R, respectively equal to

$$\begin{cases} Re\left[Z_R\right] = \dfrac{\omega^4 C_S^2 L_M^2 R_L}{\left(\omega^2 C_S L_S - 1\right)^2 + \omega^2 C_S^2 R_L^2} \\ Im\left[Z_R\right] = \dfrac{-\omega^3 C_S^2 L_M^2 \left(\omega^2 C_S L_S - 1\right)}{\left(\omega^2 C_S L_S - 1\right)^2 + \omega^2 C_S^2 R_L^2} \end{cases} \tag{4}$$

If the working pulsation is equal to $\omega = \omega_S = \sqrt{(\frac{1}{L_S C_S})}$, the following conditions are obtained.

$$\begin{cases} Re\left[Z_{R0}\right] = \dfrac{\omega_S^2 L_M^2}{R_L} \\ Im\left[Z_{R0}\right] = 0 \end{cases} \tag{5}$$

Then, the total input impedance can be calculated as

$$Z_T = Z_{LP} + Z_R = j\omega L_{LP} + \frac{1}{j\omega C_P} + Z_R \tag{6}$$

and superimposing the condition $Im[Z_T](\omega = \omega_s) = 0$, the value of C_P s is equal to

$$C_P = \frac{1}{\omega_s^2 L_P}. \tag{7}$$

In such condition, $f = 2\pi\omega_S$ is a frequency able to realize a ZPA between the input current and voltage. In order to verify if this frequency is unique, the operating pulsation ω and the input total impedance are normalized respectively on the secondary side pulsation ω_S and on the real part of the reflected impedance in the condition $\omega = \omega_S$, $Re[Z_{R0}]$ as follow:

$$u = \frac{\omega}{\omega_S}, \qquad Z_n = \frac{Z_T}{Re[Z_{R0}]}. \tag{8}$$

The main goal of the compensation is the power transfer maximization. For this reason, the imaginary part of the normalized total input impedance Z_n, whose expression is shown in (9) has to be equal to zero.

$$Im[Z_n] = -\frac{1}{\omega C_P (Re[Z_{R0}])} + \frac{\omega L_P}{Re[Z_{R0}]} + \frac{Im[Z_R]}{Re[Z_{R0}]}. \tag{9}$$

By the use of the primary side quality factor Q_P and the secondary side quality factor Q_S, whose expressions are reported in (10), each single term composing the imaginary part of the impedance Z_n can be expressed as in (11), (12), (13).

$$Q_P = \frac{L_P R_L}{\omega_S L_M^2} \qquad Q_S = \frac{L_S \omega_S}{R_L} \tag{10}$$

$$\frac{1}{\omega C_P (Re[Z_{R0}])} = \frac{Q_P}{u} \tag{11}$$

$$\frac{\omega L_P}{Re[Z_{R0}]} = u Q_P \tag{12}$$

$$\frac{Im[Z_R]}{Re[Z_{R0}]} = \frac{u^4}{\left(u^2 - 1\right)^2 Q_S^2 + u^2} \tag{13}$$

The expression of the imaginary part of Z_n can be then reformulated in:

$$Im[Z_n] = \frac{u^2 - 1}{D(Q_P, Q_S, u)} P(Q_P, Q_S, u). \tag{14}$$

The expression of $D(Q_P, Q_S, u)$ is equal to

$$D(Q_P, Q_S, u) = u(u^2 - 1)^2 Q_S^2 + u^3 \tag{15}$$

while, $P(Q_P, Q_S, u)$ is a 4-th order polynomial expressed as the following equation

$$P(Q_P, Q_S, u) = \alpha_4 u^4 + \alpha_2 u^2 + \alpha_0, \tag{16}$$

in which the coefficients are:

$$\alpha_4 = Q_P Q_S^2 - Q_S, \tag{17}$$

$$\alpha_2 = Q_P - 2Q_P Q_S^2, \tag{18}$$

$$\alpha_0 = Q_P Q_S^2. \tag{19}$$

Normally, Q_P and Q_S values are greater than one, then the coefficient α_4 is greater than zero. As a consequence, $P(Q_P, Q_S, u) > 0$ if the polynomial discriminant $\Delta < 0$. Applying then the condition

$$\alpha_2^2 - 4\alpha_4\alpha_0 < 0 \tag{20}$$

and substituting the coefficient values shown in (17), (18), (19) in (20), it is possible to find the condition for which the frequency $f = 2\pi\omega_s$ is the only one guaranteeing the ZPA, as reported in (21)

$$Q_P > K_C, \tag{21}$$

in which

$$K_C = \frac{4Q_S^3}{4Q_S^2 - 1}. \tag{22}$$

III. Coupled DD Coils Modeling

Among the different coils architectures, usually employed in the RIPT systems, the DD structure is chosen for its advantages. In particular, it is characterized by high misalignment tolerances and reduced border effects. Besides, thanks to the employment of DD coils, higher self-inductance values are reachable if compared to other coil typologies with the same dimensions. The coil geometric structure can be approximated to a set of N linear conductors linked by a continuity constraint. For this reason, a coil can be uniquely defined by a matrix having dimensions $(N+1, 3)$, whose elements are the extreme space coordinates of the N linear conductors composing the antenna. The principle of superposition can be applied, then the self-inductance and the mutual inductance values can be calculate as

$$L \quad (\text{or } L_M) = \frac{\mu}{I} \sum_{i,j=1}^{N} iV_{i,j} \tag{23}$$

in which μ is the magnetic permeability, I is a reference current and $iV_{i,j}$ are the potential vectors induced by the *i-th* elements on the *j-th* elements composing the coil for the self-inductance evaluation, or the potential vectors induced by the *i-th* elements composing the transmitter on the *j-th* elements composing the receiver in the case of the mutual inductance calculation.

In particular, the self-induced potential can be calculated with the exact formula, while the potential induced by the $i-th$ element on the $j-th$ element can be approximated as the product between the potential vector on the midpoint of the induced element and the geometrical projection of the induced element on the inducing one.

IV. Iterative algorithm implementation

The presented iterative algorithm, whose purpose is the bifurcation-free coils sizing, is implemented in MATLAB environment. It is based on the initial definition of the load condition and the desired coils dimensions. In particular, the input data of the algorithm are: the coil wire section s_c, the maximum space between turns $d_{t,max}$, the desired gap between coils g_c, the desired coils external dimensions l_c and w_c, the load value R_L and the chosen operating resonant frequency f_R.

The coils are drawn by following the principle reported in Section III, the number of turns n_t is initialized to 1. Then, the self-inductance and the mutual inductance values are calculated as in (23). The bifurcation-free condition expressed in (21) is imposed to verify the uniqueness of the chosen resonant frequency. If the condition is verified, the algorithm stops, otherwise n_t is increased by winding a turn inwards. Then the process is re-iterated. If the the number of turns is the maximum allowable, it is set to 1 and the distance between turns is decreased to repeat the process. If d_t is the minimum allowable and equal to the wire diameter, the desired external dimensions are increased and the process is repeated. As for the geometrical design, the outputs of the algorithm are the effective external dimensions, the effective number of turns and the distance between turns. As for the electrical design, the outputs of the model are the self-inductance and the mutual inductance values and the capacitance value of the compensation networks. In Fig. 2, a flowchart of the presented algorithm is shown.

The main advantage of applying this algorithm is the low computational effort. As a matter of fact, although the iteration process may require a high execution time, the operations performed are uniquely algebraic. In contrast, the magneto-static models, commonly used for coil sizing, are based on integral-differential equations, requiring higher computational efforts.

V. Validation

By applying the design method described in the previous section, a pair of DD antennas are designed. A resonant frequency $f_R = 100$ kHz is chosen. The coils are sized for a mutual distance equal to 6 centimeters and a load $R_L = 15\ \Omega$. The designed coils are shown in Fig. 3 and their characteristics are reported in Table I.

In Fig. 4, the trend of the mutual inductance as a function of misalignment is shown. The mutual inductance value is obviously maximum in the absence of

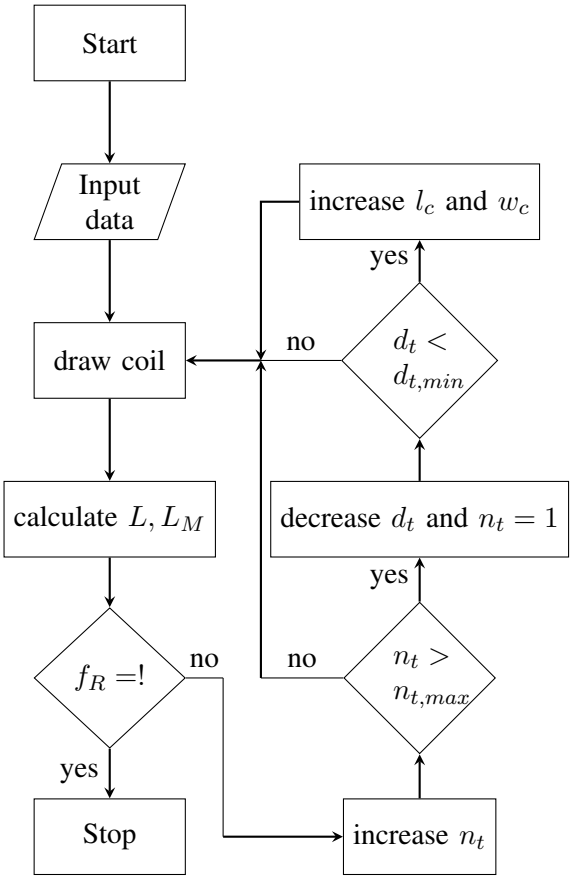

Fig. 2. Coils design algorithm flowchart

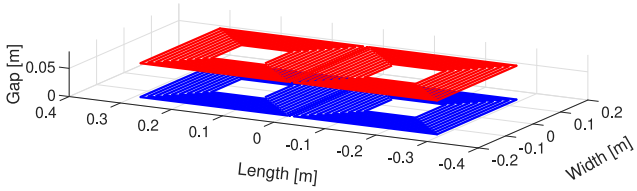

Fig. 3. Designed DD coils.

TABLE I
COILS CHARACTERISTICS

l_c [cm]	w_c [cm]	d_t [cm]	s_c [mm^2]	N_t [$-$]	L [μH]	M [μH]
58	29	1	2.5	10	60.18	23

misalignment, therefore the bifurcation-free condition is verified for this value. Considering (21), the bifurcation phenomenon can not occur for any other coils reciprocal position.

For the validation, the internal resistance of the coils is also considered and it is equal to $R_P = R_S = 0.41\ \Omega$. The compensation network capacitance value is equal to $C_P = C_S = 42.09$ nF. Fig. 5 shows the imaginary part of the total input impedance Z_T as function of the operating

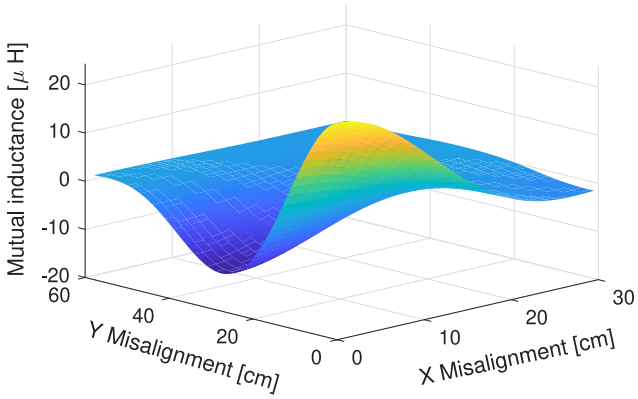

Fig. 4. Mutual inductance trend as function of misalignment.

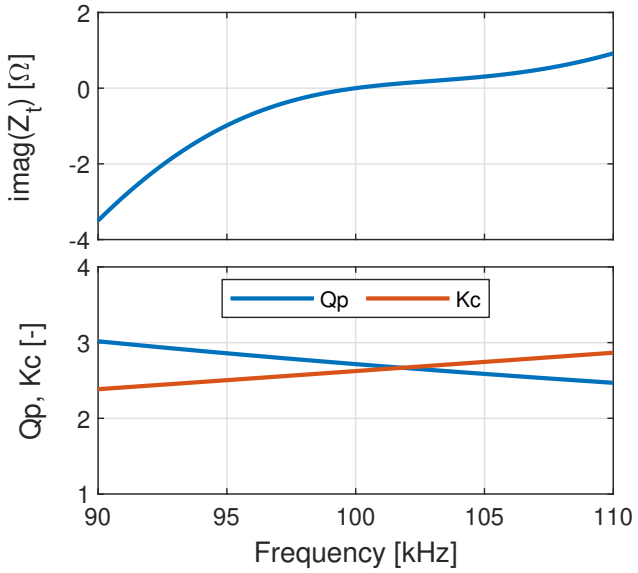

Fig. 5. Imaginary part of the input total impedance as function of frequency, comparison between Q_P and K_C.

frequency. As it can be seen, at $f = f_R$, the total input impedance is purely real and the chosen frequency is the only one guaranteeing the ZPA between the input voltage and current. The comparison between Q_P and K_C is also shown.

In order to validate the proposed design method, a system simulation was carried out in PLECS environment. Fig. 6 shows the full schematic of the system. It is composed of a voltage generator, a primary side inverter, the IPT system, a diode rectifier and a resistive load. The Phase Shift Modulation (PSM) is implemented on the primary side inverter to generate the AC voltage and current at the required operating frequency. $V_i = 48$ V is the input voltage, $C_1 = 10$ mF is the inverter input capacitance value and $C_2 = 2$ mF is the rectifier output capacitance value.

In Fig. 7 the primary side voltage and current are shown. As it is possible to notice, the ZPA between

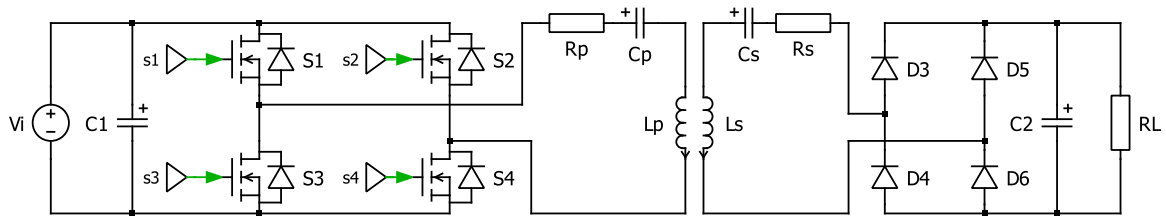

Fig. 6. PLECS schematic diagram of the RIPT system.

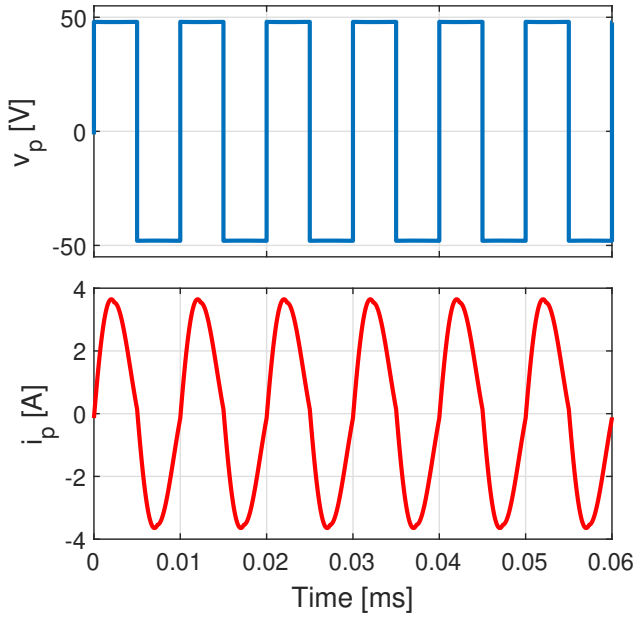

Fig. 7. Primary side voltage and current.

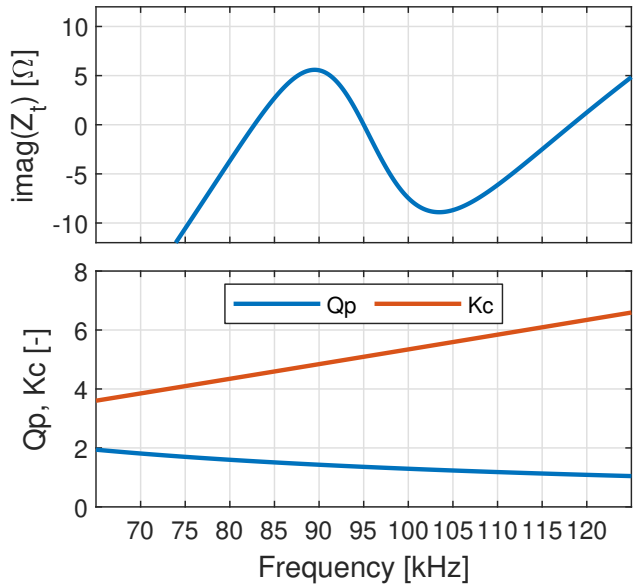

Fig. 8. Imaginary part of the input total impedance as function of frequency, comparison between Q_P and K_C with half load condition.

voltage and current is ensured. Additionally, the system is simulated with a load value equal to the half of the design value and the bifurcation-free condition is evaluated. As result of the theoretical analysis, the bifurcation-free condition is not verified, as it is possible to notice in Fig. 8 in which is clearly notable that $f_R = 100$ kHz is not the unique resonant frequency and $Q_P < K_C$ at $f_R = 100$ kHz. The results of the theoretical analysis are confirmed by the simulations. In Fig. 9 primary side voltage and current with a load value equal to the half of the design one are shown. It is possible to notice how the current is affected by a considerable distortion due to the bifurcation phenomenon.

VI. Conclusions

In this paper, a method for bifurcation-free design of an RIPT system has been presented. In particular, a Series-Series compensated system based on DD coils has been considered. A theoretical study of the bifurcation condition has been performed, and an iterative procedure for the coil sizing has been presented. It is based on the construction of the coils by evaluating the potential

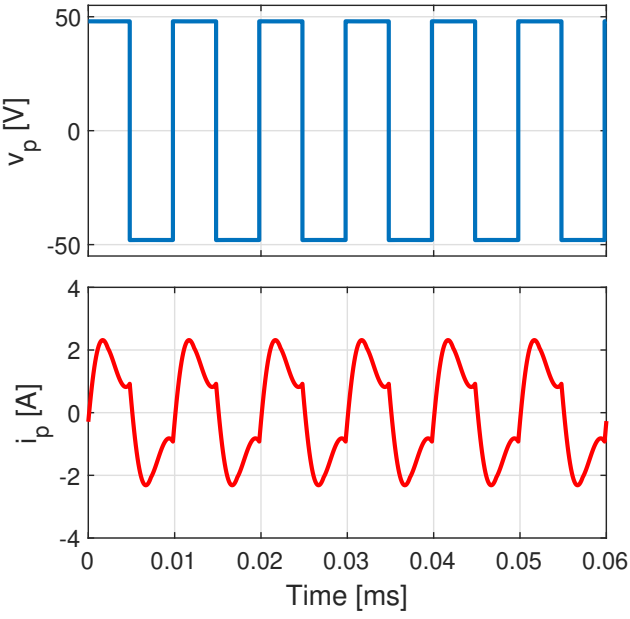

Fig. 9. Primary side voltage and current with half load.

vector of each element composing the coil and verifying the bifurcation-free condition. Simulations have been performed on the system in both bifurcation and non-bifurcation condition. The proposed method is based uniquely on the resolution of algebraic equations, unlike most of the models proposed in the literature, involving complex finite element analysis and the resolution of integral-differential equations. The simulation results showed the effectiveness of the proposed approach. As a future development, the experimental validation will be performed.

ACKNOWLEDGMENT

This work was financially supported by PON R& I 2015-2020 "Propulsione e Sistemi Ibridi per velivoli ad ala fissa e rotante – PROSIB", CUP no:B66C18000290005, by H2020-ECSEL-2017-1-IA - two-stage "first and european sic eightinches pilot line-REACTION", by Prin 2017- Settore /Ambito di intervento: PE7 linea C - Advanced power-trains and -systems for full electric aircrafts, by PON R& I 2014-2020 - AIM (Attraction and International Mobility), project AIM1851228-1.

REFERENCES

[1] M. Longo, D. Zaninelli, F. Viola, P. Romano, R. Miceli, M. Caruso, and F. Pellitteri, "Recharge stations: A review," in *2016 Eleventh International Conference on Ecological Vehicles and Renewable Energies (EVER)*, 2016, pp. 1–8.

[2] R. Miceli and F. Viola, "Designing a sustainable university recharge area for electric vehicles: Technical and economic analysis," *Energies*, vol. 10, no. 10, 2017.

[3] Z. Zhang, H. Pang, A. Georgiadis, and C. Cecati, "Wireless power transfer—an overview," *IEEE Transactions on Industrial Electronics*, vol. 66, no. 2, pp. 1044–1058, 2019.

[4] F. Pellitteri, A. O. Di Tommaso, and R. Miceli, "Investigation of inductive coupling solutions for e-bike wireless charging," in *2015 50th International Universities Power Engineering Conference (UPEC)*, 2015, pp. 1–6.

[5] H. MEŞE and M. Anılcan BUDAK, "Efficiency investigation of a 400w resonant inductive wireless power transfer system for underwater unmanned vehicles," in *2020 IEEE Wireless Power Transfer Conference (WPTC)*, 2020, pp. 223–226.

[8] M. Caruso, A. O. Di Tommaso, R. Miceli, C. Nevoloso, C. Spataro, and F. Viola, "Interior permanent magnet synchronous motors: Impact of the variability of the parameters on their efficiency," in *2016 IEEE International Conference on Renewable Energy Research and Applications (ICRERA)*, 2016, pp. 1163–1167–.

[6] S. Ansari, A. Das, and A. Bhattacharya, "Resonant inductive wireless power transfer of two-coil system with class-e resonant high frequency inverter," in *2019 6th International Conference on Signal Processing and Integrated Networks (SPIN)*, 2019, pp. 269–273.

[7] M. Caruso, A. Di Tommaso, M. Lombardo, R. Miceli, C. Nevoloso, and C. Spataro, "Maximum torque per ampere control algorithm for low saliency ratio interior permanent magnet synchronous motors," in *2017 IEEE 6th International Conference on Renewable Energy Research and Applications (ICRERA)*, 2017, pp. 1186–1191.

[9] F. Pellitteri, V. Boscaino, A. O. Di Tommaso, R. Miceli, and G. Capponi, "Wireless battery charging: E-bike application," in *2013 International Conference on Renewable Energy Research and Applications (ICRERA)*, 2013, pp. 247–251.

[10] H. Yu, G. Zhang, L. Jing, Q. Liu, W. Yuan, Z. Liu, and X. Feng, "Wireless power transfer with hts transmitting and relaying coils," *IEEE Transactions on Applied Superconductivity*, vol. 25, no. 3, pp. 1–5, 2015.

[11] T. Wang and C. Zhao, "Analyses on superposition action in diagonal dd coils to intensify ipt power capacity," in *2018 IEEE International Conference on Mechatronics and Automation (ICMA)*, 2018, pp. 966–972.

[12] Y. H. Sohn, B. H. Choi, E. S. Lee, G. C. Lim, G. Cho, and C. T. Rim, "General unified analyses of two-capacitor inductive power transfer systems: Equivalence of current-source ss and sp compensations," *IEEE Transactions on Power Electronics*, vol. 30, no. 11, pp. 6030–6045, 2015.

[13] C. Fang, J. Song, L. Lin, and Y. Wang, "Practical considerations of series-series and series-parallel compensation topologies in wireless power transfer system application," in *2017 IEEE PELS Workshop on Emerging Technologies: Wireless Power Transfer (WoW)*, 2017, pp. 255–259.

[14] M. Iordache, L. Mandache, D. Niculae, and L. Iordache, "On exact circuit analysis of frequency splitting and bifurcation phenomena in wireless power transfer systems," in *2015 International Symposium on Signals, Circuits and Systems (ISSCS)*, 2015, pp. 1–4.

[15] X. CHEN, W. LU, Y. DONG, and H. JIANG, "Magnetizer optimization of dd type coils for ev wireless charging system," in *2019 22nd International Conference on Electrical Machines and Systems (ICEMS)*, 2019, pp. 1–4.

[16] A. O. Di Tommaso, F. Genduso, and R. Miceli, "A small power transmission prototype for electric vehicle wireless battery charge applications," in *2012 International Conference on Renewable Energy Research and Applications (ICRERA)*, 2012, pp. 1–6.

[17] F. Pellitteri, V. Boscaino, A. O. Di Tommaso, F. Genduso, and R. Miceli, "E-bike battery charging: Methods and circuits," in *2013 International Conference on Clean Electrical Power (ICCEP)*, 2013, pp. 107–114.